International Geology Review

ISSN: 0020-6814 (Print) 1938-2839 (Online) Journal homepage: http://www.tandfonline.com/loi/tigr20

Petrogenesis of Ilmenite-Bearing Symplectite Xenoliths from Vitim Alkaline Basalts and Yakutian Kimberlites, Russia

Konstantin D. Litasov , Vladimir G. Malkovets , Sergey I. Kostrovitsky & Lawrence A. Taylor

To cite this article: Konstantin D. Litasov , Vladimir G. Malkovets , Sergey I. Kostrovitsky & Lawrence A. Taylor (2003) Petrogenesis of Ilmenite-Bearing Symplectite Xenoliths from Vitim Alkaline Basalts and Yakutian Kimberlites, Russia, International Geology Review, 45:11, 976-997, DOI: 10.2747/0020-6814.45.11.976

To link to this article: http://dx.doi.org/10.2747/0020-6814.45.11.976

Published online: 14 Jul 2010.

International Geology Review, Vol. 45, 2003, p. 976–997.

Petrogenesis of Ilmenite-Bearing Symplectite Xenoliths from Vitim Alkaline Basalts and Yakutian Kimberlites, Russia

KONSTANTIN D. LITASOV,[1]

Institute of Mineralogy, Petrology, and Economic Geology, Tohoku University, Sendai 980-8578, Japan

VLADIMIR G. MALKOVETS,

Institute of Mineralogy and Petrography, Siberian Branch, Russian Academy of Sciences, Novosibirsk, 630090, Russia and Planetary Geosciences Institute, Department of Earth and Planetary Sciences, University of Tennessee, Knoxville, Tennessee 37996

SERGEY I. KOSTROVITSKY,

Institute of Geochemistry, Russian Academy of Sciences, Irkutsk 664033, Russia

AND LAWRENCE A. TAYLOR

Planetary Geosciences Institute, Department of Earth and Planetary Sciences, University of Tennessee, Knoxville, Tennessee 37996

Abstract

Ilmenite-bearing symplectite, typically ilmenite-clinopyroxene, occurs in rare mantle xenoliths from kimberlite and other alkaline rocks. Two major hypotheses have been proposed for their origin: (1) exolution from high-pressure pyroxene or garnet; and (2) cotectic or eutectic co-precipitation from evolved "proto-kimberlite" melt, producing megacrysts. Here we present new findings about these ilmenite-clinopyroxene symplectites in the Miocene picrobasalts and Pleistocene basanites of the Vitim volcanic field, central Siberia. For comparison, we have described unusual ilmenite-clinopyroxene symplectites from Yakutian kimberlites: the Mary pipe (Kuoisk field) and the Mir pipe (Malo-Botuobinsk field).

Symplectite clinopyroxene from Vitim alkaline basalts corresponds to the low-Mg end of the clinopyroxene megacryst trend. They have an Mg# of 70–72 and contain 1.5–2.0 wt% TiO_2. Ilmenites from Vitim symplectites are Cr-poor and contain 5.3–6.3 wt% MgO, whereas ilmenites from kimberlite symplectites contain 0.1–1.4 wt% Cr_2O_3 and 8–13 wt.% MgO. However, trace-element patterns of symplectitic clinopyroxene in both kimberlites and alkaline basalts are similar. Clinopyroxenes from Vitim symplectites have more evolved trace-element patterns (Lan = 3.1–3.8, normalized to primitive mantle) relative to the majority of megacrysts (Lan = 1.0–3.8). Modeling of fractional crystallization of clinopyroxene from alkaline basaltic melt indicates that clinopyroxenes from symplectites correspond to the residual melt fraction of 20–40%, which is high for eutectic crystallization.

Symplectites from the Mary pipe can be divided into Cr-rich ($Cr_2O_3^{cpx}$ = 0.20–0.39 wt.% and $Cr_2O_3^{ilm}$ = 0.7–1.3 wt%) and Cr poor ($Cr_2O_3^{cpx}$ = 0.04–0.16 wt.% and $Cr_2O_3^{ilm}$ = 0.1–0.4 wt.%) subgroups. However trace-element patterns in clinopyroxenes from both groups of symplectites are similar. This may indicate a symplectite origin from different pulses of magma. Cr-enrichment in the Cr-rich group can be related to contamination by adjacent peridotites.

Compositional and textural variations in symplectites from both the alkaline basalts and kimberlites reveal similarities in genesis and a clear connection with megacryst assemblages. We suggest that ilmenite-clinopyroxene symplectites characterize the initial stage of simultaneous precipitation of ilmenite and clinopyroxene. They crystallize after the majority of the clinopyroxene megacrysts and before normal Ilm-Cpx intergrowths and ilmenite megacrysts. This indicates a possible cotectic rather than eutectic precipitation of ilmenite and clinopyroxene in symplectites.

Pressure and temperature estimations indicate that Ilm-Cpx symplectites from the Mir and Mary kimberlite pipes formed at pressures of 40–50 kbar, whereas those from Vitim basalts formed at lower pressures of 12–17 kbar. Coexisting Fe-Ti oxides in Vitim ilmenites from symplectites and megacrysts suggest equilibration temperatures of 690–1025°C at fO_2 = 0.22–1.88 log units below the QFM buffer. This redox state is similar to that of spinel peridotites in the same localities.

[1]Corresponding author; email: klitasov@ganko.tohoku.ac.jp

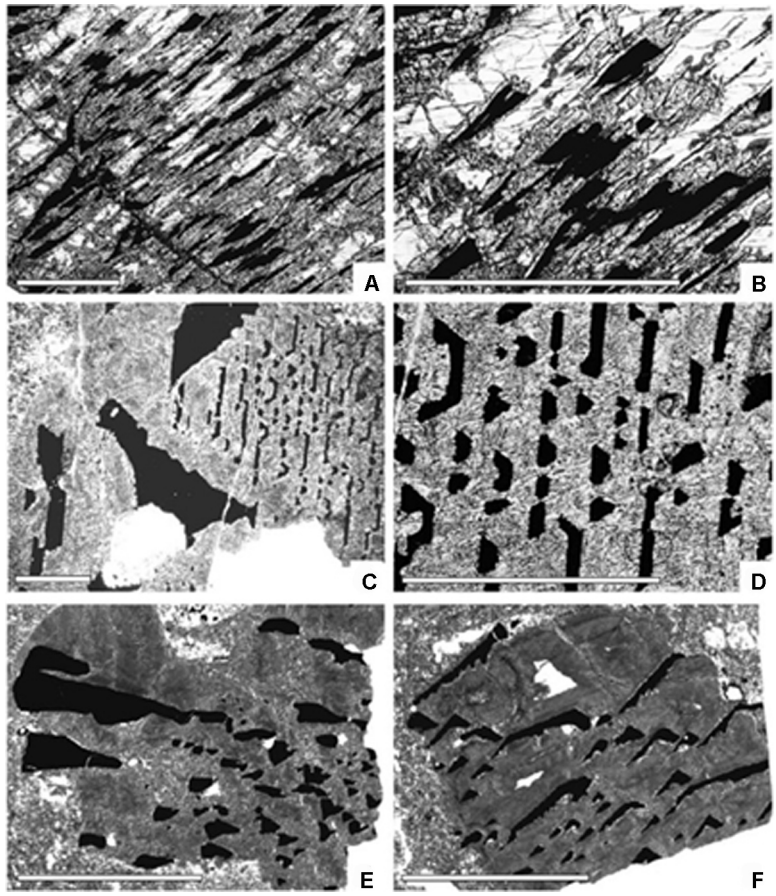

FIG. 1. Photomicrographs of ilmenite-clinopyroxene symplectites from Vitim alkaline basalts. A. Irregular elongated plates of ilmenite (black) in a clinopyroxene matrix (sample VPS-2 from the Miocene picrobasalts). Clinopyroxene is partially recrystallized along grain boundaries. Brown glass is observed in interstices. B. Enlargement of A. C. Symplectite from the Pleistocene basanites, sample VBS-3. D. Enlargement of C, showing replacement of clinopyroxene by a secondary assemblage of orthopyroxene, clinopyroxene, magnetite, plagioclase, and glass. E and F. Samples VBS-1 and VBS-2, respectively, cut perpendicular and obliquely to the elongation of the ilmenite. Scale bar is 5 mm.

Introduction

ILMENITE-CLINOPYROXENE symplectites (also termed "graphic" or lamellar intergrowths) are rare among xenoliths from kimberlite (Dawson and Reid, 1970; Ringwood and Lovering, 1970; Garrison and Taylor, 1981; Kostrovistky and Piskunova, 1989). They are also scarce among xenoliths from other alkaline rocks, such as alnoites from Malaita Island, South Pacific (Nixon and Boyd, 1979) or minettes from the Thumb, Colorado Plateau (Ehrenberg, 1982). These symplectities consist of large, single, optically continuous clinopyroxene crystals with intergrown ilmenite, commonly in the form of ruids, making for a graphic texture (Fig. 1). Earlier, mechanisms for the formation of such symplectites were extensively discussed, and several hypotheses have been proposed: (1) exolution from a high-pressure form of Ti-rich pyroxene or garnet (Dawson and Reid, 1970; Ringwood and Lovering, 1970); (2) replacement of pyroxene by ilmenite (Frick, 1973); (3) eutectic crystallization (Gurney et al., 1973; Boyd and Nixon, 1973; Wyatt, 1977); and (4) cotectic precipitation (Frick, 1973). Most researchers considered that ilmenite-silicate symplectites formed by co-precipitation from "proto-kimberlite"

liquid, in relationship with Cr-poor megacryst assemblages, based on the similarities in mineral chemistry and coexistence with more common ilmenite intergrowths (Gurney et al., 1973; Nixon and Boyd, 1979; Garrison and Taylor, 1981). However, there is reason to question many of these ideas based upon new discoveries.

Ilmenite-clinopyroxene (Ilm-Cpx) symplectites occur among xenoliths in alkaline basalts of the Vitim volcanic field (Litasov et al., 1998). They were found in Pleistocene (1.0–1.5 Ma) basanites from the Bulykhta River (Litasov and Ashchepkov, 1996; Litasov and Litasov, 1999a) and in Miocene (14–16 Ma) picrobasalts (MgO = 14–16%, $Na_2O + K_2O$ = 2.2–3%) from the Bereya Quarry, the well-known locality with a unique diversity of xenoliths, including garnet peridotites (e.g., Ionov et al., 1993; Litasov et al., 2000; Litasov and Taniguchi, 2002). For a comparative study, we compiled data on unusual symplectite xenoliths from Yakutian kimberlites (the Mary pipe, Kuoisk field, and the Mir pipe, Malo-Botuobinsk field; see Sobolev and Nixon, 1987 and Griffin et al., 1999 for field locations). Ilm-Cpx symplectites from the Mary pipe are unusual in that they form two compositional groups, Cr-rich and Cr-poor (Kostrovitsky and Piskunova, 1989). Gt-bearing Ilm-Cpx symplectites from the Mir pipe possess a complex history of deformation and recrystallization, after formation of the symplectite aggregates. The purpose of this study is to re-evaluate the possible models and conditions for the origin of Ilm-Cpx symplectites, based on new mineralogical and major- and trace-element data on a Siberian suite of symplectite samples.

Analytical Methods

Major elements in the symplectites and other xenolith and megacryst minerals were measured with a JEOL Superprobe JXA-8800 microanalyzer at Tohoku University in Sendai, Japan and by a Camebax Micro-analyzer in Novosibirsk, both based on standard electron-microprobe techniques, with an operating voltage of 20 kV, 40 nA sample current, and 1–10 μm beam size. Natural and synthetic minerals and oxides were used as standards, and probe data were corrected for ZAF effects. Trace elements in minerals were determined using a Cameca IMS 4f ion probe at the Institute of Microelectronics (IMAN), Yaroslavl', Russia, using energy-filtering techniques (Shimizu and Hart, 1982). The spectra were accumulated during five cycles with a total of 50–60 minutes counting time. Details of the analytical procedures are given by Sobolev et al. (1996) and Batanova et al. (1998). Precision and accuracy are within 10% for values above 0.1 ppm, and within 40% for concentrations below 0.1 ppm.

Petrography

Symplectites from Vitim alkaline basalts

Seven samples of the Ilm-Cpx symplectites were recovered from the Vitim volcanic field. Two samples were from Miocene picrobasalts of Bereya Quarry and five from Pleistocene basanites at the Bulykhta outcrop (see Litasov et al., 2000 and Litasov and Taniguchi, 2002, for locations). Ilmenite and clinopyroxene megacrysts and common Ilm + Cpx ± biotite and Ilm-biotite intergrowths are abundant at both localities. The modal abundance of ilmenite in symplectites ranges from 15 to 30%, whereas the modal proportions of clinopyroxene and ilmenite in the common intergrowths vary considerably. The Ilm-Cpx symplectites range in size from 2 to 6 cm. These each consist of an optically continous single crystal of clinopyroxene.

The ilmenite plates in Bereya symplectites (Fig. 1A) are coarser (0.5–5.0 mm) than those from Bulykhta. They have a homogeneous inner structure and are irregular in shape. The clinopyroxene is mostly fresh, but has recrystallyzation rims along cleavage fractures and along contact with ilmenite plates. Recrystallized clinopyroxene also coexists with Ti-rich brown glass (Fig. 1B).

The size of the ilmenite plates in the Bulykhta symplectites varies from 0.03 to 1.5 mm. Euhedral plates of Ti-biotite occur in the boundary zone of one symplectite (VBS-1). In cross-section (Figs. 1C–1D), the ilmenite plates have skeletal hexagonal and triangle shapes. Coarse plates of ilmenite have recrystallized and consolidated into larger euhedral grains (up to 1 cm in size), which have no preferred orientation (Fig. 1E). Coarse ilmenite ruids commonly form fine-grained blocks with a graphic texture (Fig. 1C). Ilmenite plates, in turn, consist of a two-phase intergrowth, with the ilmenite matrix containing Ti-magnetite lamella, similarly to discrete ilmenite megacrysts from the same locales (Litasov and Ashchepkov, 1996). Orientation of the Ti-magnetite lamellae invariably coincides with orientation of the host ilmenite plates within the symplectite. The clinopyroxene in most of the samples has been partially replaced by vermicular aggregates of

secondary clinopyroxene, orthopyroxene, Ti-magnetite, plagioclase, and glass (Figs. 1C–1F).

Symplectites from Yakutian kimberlites

The Ilm-Cpx symplectites from the Mary and Mir kimberlites (Fig. 2) are generally similar to those from the Bulykhta (Vitim) and represent classic graphic-textured intergrowths, which have been described previously (e.g., Dawson and Reid, 1970; Ringwood and Lovering, 1970). Clinopyroxene from the Mary symplectites exhibits practically no alteration, whereas clinopyroxene from the Mir typically has spongy rims, similar to those shown in Figure 1A and locally replaced by secondary serpentine, chlorite, and calcite. The symplectites from the Mary and Mir pipes range in size from 1 to 8 cm.

Sample K-78 from the Mir pipe, described originally by Kostrovitsky et al. (1992), has a unique heterogeneous texture consisting of three distinct zones: (1) fine-grained; (2) coarse-grained; and (3) a granular Ilm-Cpx aggregate. The second and third zones can also contain both coarse and fine-grained garnet (Fig. 3). The clinopyroxene has been altered extensively by fluids from the host kimberlite, and is replaced by a micro-crystalline aggregate of calcite, serpentine, and minor pyrite. Discontinuous rutile rims are present around ilmenite plates or euhedral grains. The garnet forms rims around ilmenite grains, and in turn is partially replaced by metasomatic phlogopite. Textural relationships between ilmenite and clinopyroxene are different within zones 1 and 2 (Fig. 3). Partial recrystallization has resulted in transformation of

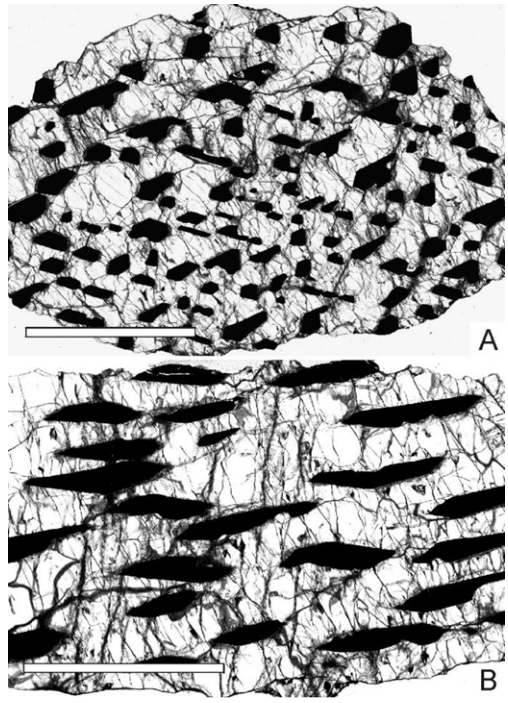

FIG. 2. Photomicrographs of ilmenite-clinopyroxene symplectites from Mary kimberlites, consisting of oriented intergrowths of ilmenite plates (black) in a matrix of pyroxene. A. Cross-section perpendicular to elongation of the ilmenite plates, sample Mer-470. B. Cross-section parallel to elongation of the ilmenite plates, sample Mer-1. Scale bar is 5 mm.

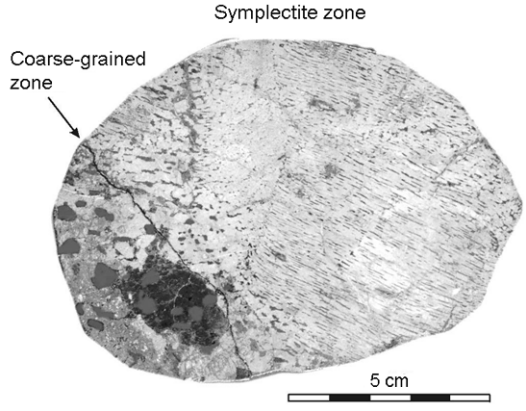

FIG. 3. Image of the composite garnet-bearing, Ilm-Cpx symplectite, sample K-78. Note the deformation of ilmenite plates along the boundaries of different symplectite blocks and equidimensional grains of ilmenite (grey) in a garnet (black)-bearing zone.

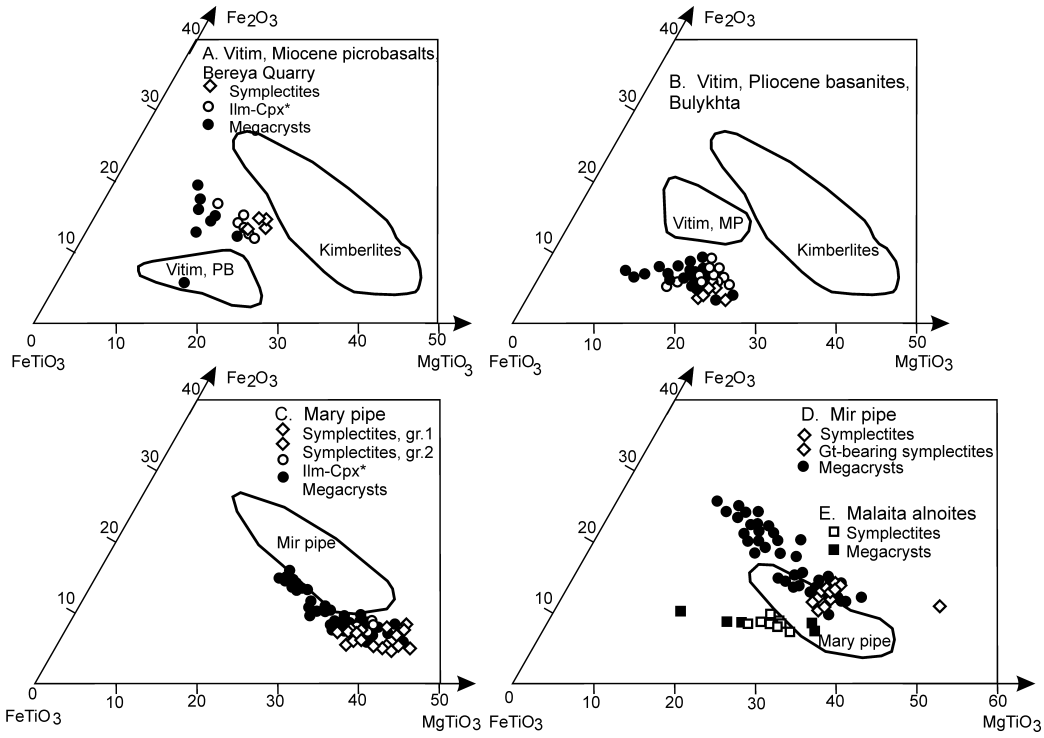

FIG. 4. Ternary plot of Fe_2O_3-$FeTiO_3$-$MgTiO_3$ showing the compositions of ilmenites from Ilm-Cpx symplectites and megacrysts. Ilm-Cpx* represents common Ilm-Cpx intergrowths.

the symplectite texture into unusual fingerprint-like myrme-kites. The presence of distinct cleavage and crushing along grain boundaries suggests intensive deformation of the sample after crystallization of the Ilm-Cpx symplectite.

Major-Element Chemistry

Symplectites from Vitim alkaline basalts

Major-element compositions of selected xenolith and megacryst phases are given in Tables 1–3. Homogenous ilmenites from Bereya symplectites can be classified as picroilmenites, and contain 20–22 mol% of $MgTiO_3$, geikilite, and 13–15 mol% Fe_2O_3, hematite. Ilmenites with these compositions occur together, with the common Ilm-Cpx intergrowths, in the Mg-rich part of ilmenite-megacryst field on Figure 4A. This statement is applicable for all suites, including ilmenites from the Bulykhta, Vitim field (Fig. 4B), Yakutian kimberlites, and Malaita alnoites (Nixon and Boyd, 1979), which were considered for comparison as an example of non-kimberlitic suite (Figs. 4C–4D). Matrix ilmenites of composite megacrysts from the Bereya Quarry fall together with matrix ilmenite from megacrysts and symplecties from Bulykhta (Fig. 4A).

All ilmenites from the Bulykhta outcrop, including Ilm-Cpx symplectite, common intergrowths, and megacrysts, have two-phase textures, consisting of an ilmenite matrix and Ti-magnetite lamellae. Matrix ilmenites in the Bulykhta megacrysts and symplectites contain low Fe_2O_3 (3–7 mol%) and high TiO_2 relative to homogenous ilmenites (70–75 mol% of $FeTiO_3$, ilmenite, Table 1, Fig. 1B). Lamellar Ti-magnetite in ilmenite from symplectite is enriched in ulvöspinel ($Mt_{22\text{-}20}Usp_{78\text{-}80}$) and contains 27–30 wt% TiO_2, 4.2–5.0 wt% MgO, and 3.2–3.9 wt% Al_2O_3. Ti-magnetites from ilmenite megacrysts have compositions of $Mt_{42\text{-}21}Usp_{58\text{-}79}$ and contains 17–28 wt% TiO_2, 2.4–5.3 wt% MgO, and 3.4–7.2 wt% Al_2O_3. Note that Ti-magnetite in the host basanite itself contains low MgO (1.2–2.6 wt%) and 1.0–2.3 wt% Al_2O_3, relative to Ti-magnetite lamellae from megacrysts and symplectites (Table 1).

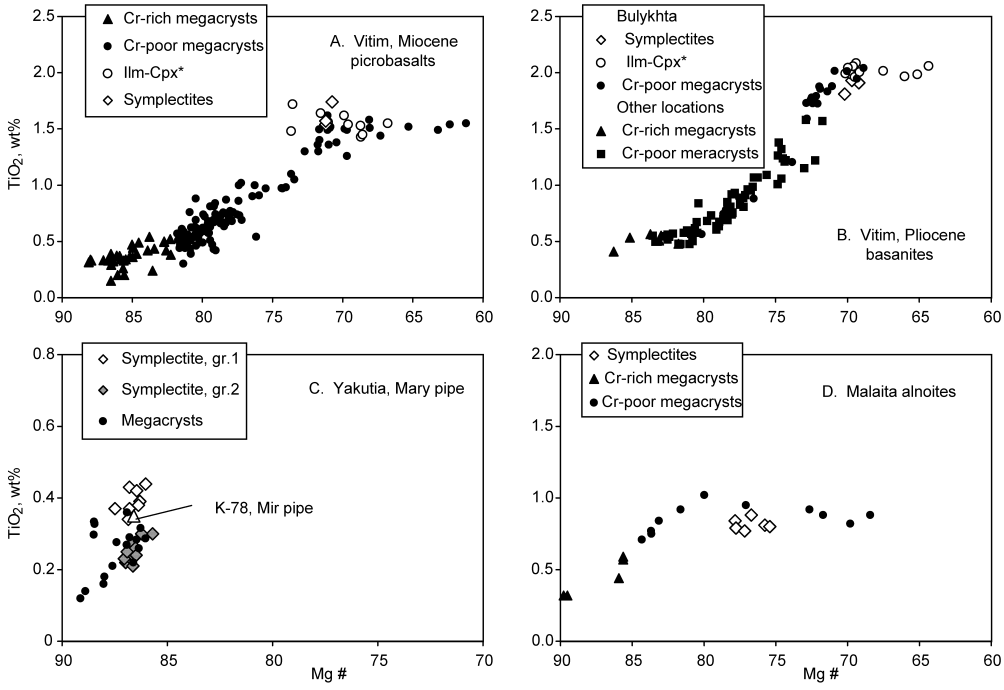

FIG. 5. Mg# versus TiO_2 in clinopyroxenes from Ilm-Cpx symplectites, megacrysts, and related xenoliths. Ilm-Cpx* represents common Ilm-Cpx intergrowths.

Rough estimations of the bulk composition of the composite ilmenite (ilmenite + Ti-magnetite lamellae) in symplectites and megacrysts indicate that the ilmenite compositions are similar for symplectites from the Bereya picrobasalt and those in the Bulykhta basanites.

Primary clinopyroxenes from the symplectites in the Vitim alkaline basalts possess homogeneous compositions (Fig. 5). Bereya symplectites have Mg# = 70.8–71.2 and contain 1.5–1.7 wt% TiO_2, 7.9–8.1 wt% Al_2O_3, and 3.1–3.2 wt% Na_2O. Clinopyroxenes from Bulykhta symplectites have Mg# = 69.2–70.2 and contain 1.8–1.9 wt% TiO_2, 8.4–8.6 wt% Al_2O_3, and 3.0–3.2 wt% Na_2O. The compositions of symplectite clinopyroxenes from both localities correspond to the most Fe-rich members of the clinopyroxene megacryst trends (Fig.5). The beginning of ilmenite precipitation is marked by an inflection in the Mg#-TiO_2 trend (Figs. 5A–5B). Clinopyroxenes from symplectites plot near the inflection, and they are generally more Mg-rich than those from common ilmenite-clinopyroxene intergrowths. Similar data were reported for other locations (Gurney et al., 1979; Schulze, 1987). For instance, a Mg#-Ti-inflection was shown for a garnet from xenoliths and megacrysts of the Monastery pipe (Schulze, 1987) and for clinopyroxenes from the Malaita alnoites (Fig. 5D) (Nixon and Boyd, 1979).

Secondary or recrystallized clinopyroxenes in symplectites contain high TiO_2 (2.0–3.5 wt%) and low Al_2O_3 (4.9–6.5 wt%) and Na_2O (0.7–1.6 wt%), relative to primary clinopyroxene in both Bereya and Bulykhta localities (Table 2). The compositions of Ti-biotite inclusions in the Bulykhta symplectite VBS-1 (Mg# = 61.1, TiO_2 = 9.7 wt%, Table 3) are similar to the discrete biotite megacrysts from the same outcrop (Mg# = 54–65, TiO_2 = 9.1–11.0 wt%; see Litasov and Litasov, 1999b; Litasov, 2000).

Symplectites from Yakutia kimberlites

Ilmenites from kimberlitic symplectites are more Mg-rich (30–44 mol% $MgTiO_3$) relative to ilmenites from alkaline basalts. Ilmenite megacrysts from the Mary and Mir kimberlite pipes form a continuous trend, with $MgTiO_3$ decreasing with increasing Fe_2O_3. Mir ilmenite megacrysts generally contain high Fe_2O_3 and low $MgTiO_3$ relative to those from the Mary pipe (Figs. 4C–4D). Similar relationships

TABLE 1. Composition of Ilmenites and Ti-Magnetites from Ilm-Bearing Symplectites and Related Rocks

Host:	Miocene picrobasalt, Bereya Quarry, Vitim field					Pliocene basanites, Bulykhta, Vitim field												
Type:	Symplectites		Ilm-Cpx[1]	Megacrysts		Symplectites						Ilm-Cpx[1]		Megacrysts				Host[2]
Sample:	VPS-1	VPS-2	V-340	PT-5	PT-1	VBS-1		VBS-2		VBS-3		BK-25		B-3		B-1		bas
Mineral	Ilm	Ilm	Ilm	Ilm	Ilm	Ilm	Ti-mt	Ilm	Ti-mt	Ilm	Ti-mt	Ilm	Ti-mt	Ilm	Ti-mt	Ilm	Ti-mt	Ti-mt
TiO_2	45.38	45.78	46.83	43.75	44.61	51.04	29.51	52.14	27.21	52.43	29.33	50.81	24.64	53.10	24.74	52.94	25.46	21.68
Al_2O_3	1.13	1.52	1.50	0.94	1.30	0.24	3.73	0.21	3.39	0.22	3.21	0.31	6.41	0.26	3.93	0.23	4.02	1.36
Cr_2O_3		0.01	0.02	0.03					0.01		0.01				0.06	0.05	0.07	0.12
Fe_2O_3	16.38	15.02	13.74	17.16	15.76	7.22	10.32	5.51	13.76	4.10	10.88	7.53	15.35	3.40	17.45	4.26	16.72	24.49
FeO	31.16	31.02	32.43	34.19	33.76	34.72	51.91	35.75	50.40	36.76	51.69	35.97	48.97	35.89	47.67	34.80	47.75	51.31
MnO	0.10	0.11	0.21	0.21	0.17	0.07	0.07	0.05	0.04	0.12	0.09	0.18	0.18	0.35	0.34	0.33	0.41	0.36
MgO	5.81	6.00	5.63	3.29	3.90	6.32	4.97	6.27	4.50	5.79	4.88	5.45	4.36	6.48	4.87	7.03	5.27	1.52
NiO	0.02	0.03		0.01	0.01		0.03		0.02		0.02				0.03		0.05	0.04
Total	99.97	99.50	100.37	99.58	99.51	99.61	100.54	99.93	99.33	99.42	100.11	100.24	99.91	99.48	99.09	99.64	99.76	100.87
Ti	0.826	0.834	0.848	0.816	0.827	0.929	0.781	0.946	0.733	0.959	0.782	0.925	0.652	0.965	0.666	0.957	0.678	0.597
Al	0.032	0.043	0.043	0.027	0.038	0.007	0.155	0.006	0.143	0.006	0.134	0.009	0.266	0.007	0.166	0.007	0.168	0.059
Cr				0.001											0.002	0.001	0.002	0.003
Fe^{3+}	0.298	0.274	0.249	0.320	0.292	0.132	0.273	0.100	0.371	0.075	0.290	0.137	0.406	0.062	0.470	0.077	0.446	0.675
Fe^{2+}	0.631	0.629	0.653	0.709	0.696	0.703	1.527	0.721	1.510	0.747	1.532	0.728	1.441	0.725	1.426	0.700	1.414	1.571
Mn	0.002	0.002	0.004	0.004	0.004	0.001	0.002	0.001	0.001	0.002	0.003	0.004	0.005	0.007	0.010	0.007	0.012	0.011
Mg	0.210	0.217	0.202	0.122	0.143	0.228	0.261	0.225	0.240	0.210	0.258	0.197	0.229	0.233	0.260	0.252	0.278	0.083
Ni	0.001	0.001					0.001		0.001		0.001				0.001		0.001	0.001
Total	2.000	2.000	2.000	2.000	2.000	2.000	3.000	2.000	3.000	2.000	3.000	2.000	3.000	2.000	3.000	2.000	3.000	3.000
Ilmenite	63.9	64.4	66.9	71.4	70.7	70.5		72.3		75.0		73.1		72.8		70.3		
Hematite	14.9	13.7	12.5	16.0	14.6	6.6		5.0		3.7		6.9		3.1		3.8		
Geikilite	21.0	21.7	20.2	12.2	14.3	22.8		22.5		21.0		19.7		23.3		25.2		
Pyrophanite	0.2	0.2	0.4	0.4	0.4	0.1		0.1		0.2		0.4		0.7		0.7		

Table continues

TABLE 1. *Continued*

Host:	Kimberlite, Mary pipe, Yakutia											Kimberlite, Mir pipe, Yakutia					
Type:	Symplectite, gr.1			Symplectite, gr.2			Gt-Ilm[1]		Megacrysts			Symplectites		Gt-symplectite[3]		Megacrysts	
Sample:	M-470	M-44	Mer-1	Mer-2	Mer-3	Mer-4	Mer-9	Mer-42	Mr-4	Mr-1	Mr-38	M-540	M-555	K-78	A-702[4]	585-1	585-3
Mineral	Ilm	Ilm	Ilm	Ilm	Ilm	Ilm	Ilm	Ilm	Ilm	Ilm	Ilm	Ilm	Ilm	Ilm	Ilm	Ilm	Ilm
TiO_2	51.71	51.87	53.39	51.19	51.85	51.02	50.50	51.00	45.67	48.49	51.19	47.05	47.68	48.63	50.55	41.74	47.27
Al_2O_3	0.97	1.15	0.75	0.51	0.80	0.60	0.50	0.54	0.11	0.20	0.47	0.74	0.70	0.71	0.80	0.69	0.63
Cr_2O_3	0.88	0.91	0.98	0.22	0.11	0.23	0.26	0.22	1.04	0.36	0.32	0.20	0.08	0.13	1.14	0.55	0.14
Fe_2O_3	7.59	8.97	5.70	9.07	6.29	10.17	10.14	9.76	16.27	11.71	8.76	15.90	15.04	13.05	12.90	23.08	15.45
FeO	25.37	25.07	25.28	28.61	26.51	27.19	27.28	28.42	29.59	29.77	28.68	26.11	27.63	28.48	20.87	29.24	28.79
MnO	0.25	0.23	0.26	0.30	0.24	0.26	0.25	0.21	0.48	0.25	0.13	0.18	0.21	0.24	0.22	0.16	0.19
MgO	11.87	12.20	12.71	9.84	12.14	10.60	10.20	9.82	6.72	8.06	10.05	9.41	8.81	8.87	13.93	5.52	7.99
V_2O_5	0.17	0.19	0.14	0.13	1.14	0.13			0.21	0.44	0.30			0.24			
NiO	0.16	0.13	0.13	0.03	0.16	0.04			0.16	0.33				0.08			
Total	98.97	100.72	99.43	99.90	99.24	100.24	99.13	99.97	100.25	99.61	99.90	99.59	100.16	100.43	100.41	100.98	100.46
Ti	0.907	0.893	0.927	0.905	0.906	0.895	0.898	0.902	0.828	0.874	0.904	0.839	0.849	0.863	0.864	0.758	0.845
Al	0.027	0.031	0.020	0.014	0.022	0.016	0.014	0.015	0.003	0.006	0.013	0.021	0.020	0.020	0.021	0.020	0.018
Cr	0.016	0.016	0.018	0.004	0.002	0.004	0.005	0.004	0.020	0.007	0.006	0.004	0.001	0.002	0.020	0.010	0.003
Fe^{3+}	0.133	0.154	0.099	0.161	0.110	0.178	0.180	0.173	0.295	0.211	0.155	0.284	0.268	0.232	0.221	0.419	0.276
Fe^{2+}	0.495	0.480	0.488	0.562	0.515	0.530	0.539	0.559	0.596	0.596	0.563	0.517	0.547	0.562	0.397	0.590	0.572
Mn	0.005	0.004	0.005	0.006	0.005	0.005	0.005	0.004	0.010	0.005	0.003	0.004	0.004	0.005	0.004	0.003	0.004
Mg	0.412	0.416	0.438	0.345	0.420	0.368	0.359	0.344	0.241	0.288	0.352	0.332	0.311	0.312	0.472	0.199	0.283
V	0.003	0.003	0.002	0.002	0.017	0.002			0.003	0.007	0.005			0.004			
Ni	0.003	0.002	0.002	0.001	0.003	0.001			0.003	0.006				0.002			
Total	2.000	2.000	2.000	2.000	2.000	2.000	2.000	2.000	2.000	2.000	2.000	2.000	2.000	2.000	2.000	2.000	2.000
Ilmenite	51.6	50.2	50.8	56.9	52.0	53.7	54.6	56.6	60.1	60.2	56.8	52.2	55.1	56.8	41.3	58.8	57.5
Hematite	6.7	7.7	4.9	8.0	5.5	8.9	9.0	8.6	14.8	10.6	7.7	14.2	13.4	11.6	11.0	21.0	13.8
Geikilite	41.2	41.6	43.8	34.5	42.0	36.8	35.9	34.4	24.1	28.8	35.2	33.2	31.1	31.2	47.2	19.9	28.3
Pyrophanite	0.5	0.4	0.5	0.6	0.5	0.5	0.5	0.4	1.0	0.5	0.3	0.4	0.4	0.5	0.4	0.3	0.4

[1]Common megacrystalline intergrowths.
[2] Ti-magnetite from basanite background.
[3] Gt-bearing Ilm-Cpx-symplectite.
[4] After Ponomarenko, 1977.

TABLE 2. Composition of Clinopyroxenes and Garnets from the Ilm-Bearing Symplectites and Related Rocks

Host:	Miocene picrobasalt, Bereya Quarry, Vitim field							Pliocene basanites, Bulykhta, Vitim field								
Type:	Symplectites			Ilm-Cpx[1]	Megacrysts			Symplectites				Ilm-Cpx[1]		Megacrysts		
Sample:	VPS-1	VPS-2	VPS-2[2]	V-340	V-184	V-167	V-161	VBS-1	VBS-2	VBS-2[2]	VBS-3[2]	BK-25	BK-21	BM-21	BM-5	BM-15
Mineral:	Cpx	Cpx	Cpx	Cpx	Cpx	Cpx	Cpx	Cpx	Cpx	Cpx	Cpx	Cpx	Cpx	Cpx	Cpx	Cpx
SiO_2	49.27	49.34	47.80	49.70	51.15	49.55	49.55	49.27	49.00	48.49	48.77	48.92	48.57	50.82	49.42	49.58
TiO_2	1.54	1.57	2.62	1.59	0.67	1.49	1.54	1.81	1.91	2.09	2.14	2.02	1.98	0.78	1.21	1.72
Al_2O_3	8.05	7.99	6.26	8.21	7.10	8.06	8.69	8.45	8.56	5.95	5.55	9.05	8.96	8.21	8.92	8.21
Cr_2O_3					0.03	0.02	0.00						0.00		0.01	
FeO	8.69	8.72	9.39	9.15	8.02	9.24	10.67	9.02	9.27	8.94	8.04	9.31	9.91	7.49	8.26	9.01
MnO	0.11	0.09	0.11	0.13	0.13	0.10	0.11	0.11	0.12	0.12	0.10	0.14	0.10	0.18	0.15	0.15
MgO	12.06	12.11	12.72	11.37	16.45	12.73	9.91	11.91	11.68	13.57	12.84	10.85	10.38	15.29	13.08	13.04
CaO	15.66	15.79	18.57	15.79	14.59	15.67	15.76	15.35	15.34	18.27	20.53	15.98	15.85	14.60	15.30	14.86
Na_2O	3.16	3.12	1.42	3.34	1.73	2.61	3.57	3.04	3.12	1.21	0.98	3.37	3.44	1.86	2.47	2.45
Total	98.54	98.74	98.89	99.28	99.87	99.47	99.80	98.96	99.00	98.64	98.94	99.63	99.20	99.23	98.82	99.03
Mg#	71.2	71.2	70.7	68.9	78.5	71.1	62.3	70.2	69.2	73.0	74.0	67.5	65.1	78.4	73.8	72.1

Host:	Kimberlite, Mary pipe, Yakutia										Kimberlite, Mir pipe, Yakutia					
Type:	Symplectite, gr.1			Symplectite, gr.2			Gt-Ilm[1]		Megacrysts		Symplectites		Gt-symplectite[3]			
Sample:	Mer-470	Mer-44	Mer-1	Mer-2	Mer-3	Mer-4	Mer-9	Mer-42	Mary-1	Mary-2	M-540	M-555	K-78	K-78	A-702[4]	A-702[4]
Mineral:	Cpx	Cpx	Cpx	Cpx	Cpx	Cpx	Gt	Gt	Cpx	Cpx	Cpx	Cpx	Cpx	Gt	Cpx	Gt
SiO_2	54.53	54.99	54.65	54.51	54.51	54.47	41.23	40.87	54.68	54.55	54.93	55.12	55.54	41.84	54.10	41.80
TiO_2	0.42	0.38	0.37	0.25	0.21	0.24	0.38	0.42	0.36	0.22	0.39	0.37	0.35	0.81	0.31	1.28
Al_2O_3	2.18	2.26	1.91	1.99	2.04	2.11	21.94	21.36	2.21	2.18	2.76	2.54	2.74	22.09	1.81	21.30
Cr_2O_3	0.28	0.30	0.34	0.13	0.14	0.10	0.20	0.29	0.3	0.07	0.14	0.07	0.05	0.11	0.08	1.13
FeO	4.95	4.95	4.59	4.41	4.70	4.65	12.16	12.78	4.73	4.53	4.96	4.84	4.57	12.27	5.48	10.70
MnO	0.11	0.10	0.09	0.10	0.13	0.11	0.50	0.48	0.13	0.07	0.14	0.13	0.15	0.36	0.17	0.17
MgO	17.73	17.60	18.00	16.42	17.09	16.69	17.99	17.23	17.62	16.43	17.03	16.78	16.55	19.05	17.60	21.00
CaO	17.55	17.61	18.06	20.39	18.69	19.78	5.00	5.34	17.71	19.81	17.11	17.43	16.81	4.16	18.00	3.12
Na_2O	1.62	1.53	1.35	1.45	1.53	1.48			1.61	1.63	1.89	2.06	2.33	0.11	1.57	0.09
Total	99.36	99.73	99.37	99.64	99.02	99.62	99.40	98.77	99.35	99.49	99.35	99.34	99.09	100.8	99.12	100.6
Mg#	86.5	86.4	87.5	86.9	87.3	86.5	72.5	70.6	86.9	86.6	86.0	86.1	86.6	72.1	85.1	77.8

[1]Common megacrystalline intergrowths.
[2]Secondary recrystallized clinopyroxene.
[3]Gt-bearing Ilm-Cpx-symplectite.
[4]After Ponomarenko, 1977.

TABLE 3. Composition of Micas from the Ilm-Cpx Symplectites and Related Rocks

Sample:	VBS-1[1]	BF[2]	K-78[3]	K-78[4]
SiO_2	35.13	35.41	40.79	41.78
TiO_2	9.74	11.12	1.78	1.43
Al_2O_3	14.34	14.29	11.93	11.87
Cr_2O_3	0.01	0.02	0.05	0.03
FeO	12.97	12.41	6.41	6.00
MnO	0.08	0.09	0.09	0.08
MgO	11.43	11.47	22.51	22.33
CaO	0.03	0.02	0.04	
Na_2O	0.57	0.58	0.51	0.43
NiO			0.10	0.09
K_2O	9.44	9.24	10.06	9.65
F	0.63	0.33	0.65	
Total	94.37	94.98	94.92	93.69
Mg#	61.1	62.2	86.2	86.9

[1]Ilm-Cpx-symplectite from Pliocene basanites, Bulykhta, Vitim field.
[2]Ti-biotite megacryst from Pliocene basanites, Bulykhta, Vitim field.
[3]Metasomatic phlogopite from Ilm-Cpx-Gt symplectite, Mir pipe, this study.
[4]Metasomatic phlogopite from Ilm-Cpx-Gt symplectite, Mir pipe, Kostrovitsky et al., 1992.

exist for symplectite ilmenites (Mir pipe, 31–34 mol% $MgTiO_3$ and 10.5–14.5 mol% Fe_2O_3; Mary pipe, 34–44 mol% $MgTiO_3$ and 4.7–10.1 mol% Fe_2O_3). Ilmenites from symplectites in both pipes correspond in composition to the most Mg-rich ilmenite megacrysts (Figs. 4C–4D).

Among Ilm-Cpx symplectites of the Mary pipe (Fig. 6), two compositional groups can be recognized. Ilmenites from Cr-rich group 1 contain 0.7–1.3 wt% Cr_2O_3. Ilmenites from Cr-poor group 2 have similar compositions with low-Cr megacrysts (Fig. 6A) and contain 0.1–0.4 wt% Cr_2O_3. Ilmenites from symplectite group 1 are also more Mg-rich (average $MgTiO_3$ = 40.7 ± 1.7 mol.%) relative to those of group 2 (average $MgTiO_3$ = 36.0 ± 2.6 mol%). Clinopyroxenes from symplectite group 2 (Mg# = 86–88; Cr_2O_3 = 0.04-0.16 wt%; TiO_2 = 0.21–0.30 wt%) form a short compositional trend similar to the discrete megacrysts (Figs. 5–6), whereas clinopyroxenes from symplectite group 1 (Mg# = 86–88; Cr_2O_3 = 0.20–0.39 wt%; TiO_2 = 0.34–0.44 wt%) have no analogues among the megacrysts (Figs. 5–6).

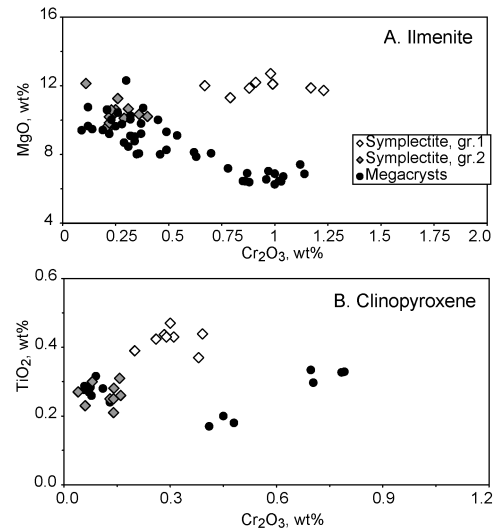

FIG. 6. Cr_2O_3 versus MgO in ilmenites and Cr_2O_3 versus TiO_2 in clinopyroxenes from the Ilm-Cpx symplectites and megacrysts of the Mary pipe.

Ilmenite from a composite garnet-bearing symplectite K-78 (Mir pipe) is similar with those from garnet-free Ilm-Cpx symplectites (31.2 mol% $MgTiO_3$, Table 1). However, Ponomarenko (1977) determined 47.2 mol% $MgTiO_3$ in ilmenite from a similar garnet-bearing Ilm-Cpx symplectite (sample A-702, Tables 1–2).

The compositions of clinopyroxene in K-78 (Mg# = 86.6; Cr_2O_3 = 0.05 wt%; TiO_2 = 0.35 wt%) are also similar with those in garnet-free Ilm-Cpx symplectites (Mg# = 86-87; Cr_2O_3 = 0.06-0.21 wt%; TiO_2 = 0.31–0.40 wt%, Table 2). They resemble also clinopyroxene from Cr-poor sympectites from the Mary pipe, whereas TiO_2 is higher.

Compositions of ilmenites and clinopyroxenes from the Mary and Mir symplectites are generally similar to those from other kimberlites of Yakutia, South Africa, and the United States (Dawson and Reid, 1970; Ringwood and Lowering, 1970; Garrison and Taylor, 1981; Mitchell, 1986). Most ilmenites contain between 30 and 44 mol% $MgTiO_3$, although Gurney et al. (1973) reported 53 mol% $MgTiO_3$ in a Riley County ilmenite.

The composition of the garnet in symplectite K-78 of the Mir pipe is generally similar to garnet from common garnet-ilmenite intergrowths and the low-Cr garnet megacrysts (Mg# = 72–83; 0.7–1.3 wt% TiO_2; 0–1.5 wt% Cr_2O_3; our unpublished data). However, the garnet from symplectite A-702, described by Ponomarenko (1977), contains high TiO_2 and Cr_2O_3 relative to that in K-78 (Table 2).

Secondary phlogopite from symplectite K-78 has Mg# = 86–87, and contains 1.4–1.8 wt% TiO_2 and 0.03–0.05 wt% Cr_2O_3. This composition is similar to phlogopites from kimberlite groundmass and megacrysts, as well as to some metasomatic phlogopites contained in mantle xenoliths from kimberlites worldwide (e.g., Delaney et al., 1980; Mitchell, 1986; Solovyova et al., 1994).

Trace-Element Chemistry

Trace-element analyses of selected clinopyroxene and garnet are listed in Table 4 and shown in Figure 7. Trace-element patterns for symplectite clinopyroxene are similar to those in all symplectites from kimberlites, and their shapes suggest clear similarities with clinopyroxenes from symplectites in alkaline basalts (Fig. 7). Clinopyroxene REE distributions from Vitim symplectites are well correlated, in megacryst assemblages, with a regular variation of major elements with decreasing Mg# (Fig. 8).

In the Bereya Quarry (Miocene picrobasalts), Cr-rich magnesian megacrysts and related pyroxenites have Mg# = 80–88. They contain low LREE (La = 1.0–1.2 ppm), Zr = 8.2–15.9 ppm) and have low (La/Yb)n = 1.2–1.5 (normalized to primitive mantle, McDonough and Sun, 1995), revealing the absence of garnet control of the HREE. Cr-poor clinopyroxene megacrysts from the central-compositional part of the megacryst suite have Mg# = 73–80. They contain medium LREE (La = 1.2–1.8 ppm), Zr = 18.6–24.6 ppm, and have high (La/Yb)n = 2.4–4.0, revealing garnet control of the HREEs. Cr-poor Ti-rich clinopyroxene megacrysts (including common Ilm-Cpx intergrowths and symplectites) have Mg# = 62–73. They also contain high LREEs (La = 1.7–2.4 ppm), Zr = 48–96 ppm, and have high (La/Yb)n = 4.0–5.6. Clinopyroxenes of most Fe-rich megacrysts and symplectites, however, have lower (La/Yb)n = 2.0–3.5, revealing probable termination of garnet crystallization.

All clinopyroxene megacrysts from Bulykhta (Pliocene basanites) have similar shape of trace-elements patterns (Fig. 7). The REE contents increase with decreasing Mg# (from La = 1.1 ppm at Mg# = 85 to La = 3.8 ppm at Mg# = 64). The (La/Yb)n ratio increases from 1.2 to 3.8 (3.1 in symplectite VBS-1).

Figure 9 shows the compositions of clinopyroxene from the modeling the fractional crystallization of the melt, which coexisted with the most primitive clinopyroxene megacryst (with lowest LREE) from the Bereya Quarry and Bulykhta. Clinopyroxene/melt partition coefficients from Hauri et al. (1994) were used for Th and Nb, with other elements from Hart and Dunn (1993). According to these calculations, the estimated residual melt fraction would be 40% for the clinopyroxene from the Ilm-Cpx symplectites of Bereya Quarry and 20–30% for those of Bulykhta.

Clinopyroxenes from megacrysts and symplectites from the Mary pipe and from symplectites from the Mir pipe have restricted trace-element variations (Fig. 7). They contain relatively high LREEs (La = 2.4–3.6 ppm), low Zr = 13–29 ppm, and have high (La/Yb)n = 4.4–7.6, thereby revealing a strong garnet control on the HREE distributions.

P-T Estimates for the Ilm-Cpx Symplectites

The exsolution temperatures for ilmenite-magnetite pairs were performed using the QUILF program et al., 1993). The exsolution temperatures

TABLE 4. Ion Probe Data for Xenolith and Megacryst Minerals, ppm

Host:	Bereya Quarry, Vitim					Bulykhta, Vitim			Mary pipe				Mir pipe	
Type:	Symplectites		Ilm-Cpx	Megacrysts[1]		Symp.	Ilm-Cpx	Meg.	Symplectites		Megacrysts		Gt-symplectite	
Sample:	PTS-2	PTS-2a	V-340	V-184	V-167	VBS-1	BK-21	BM-5	Mer-2	Mer-470	M-1	M-2	K-78	K-78
Mineral:	Cpx	Cpx	Cpx	Cpx	Cpx	Cpx	Cpx	Cpx	Cpx	Cpx	Cpx	Cpx	Cpx	Gt
Ba	0.27	3.90			0.32	0.24	0.23	0.24	0.24	0.30	0.14	0.24	0.27	0.66
Th	0.03	0.03	0.01	0.03	0.03	0.03	0.04	0.03	0.02	0.03	0.02	0.02	0.02	0.02
Nb	0.46	0.90	0.66	0.27	0.33	0.56	0.65	0.30	0.26	0.28	0.24	0.29	0.25	0.24
La	2.06	1.70	2.01	1.78	2.19	3.12	3.82	2.41	2.96	3.56	2.40	3.15	3.44	0.27
Ce	7.66	6.44	7.61	6.37	7.87	10.8	12.8	8.34	10.2	11.5	8.73	10.7	11.0	0.48
Sr	114	73.6	96.9	64.3	107	178	198	117	124	131	112	126	129	2.14
Nd	8.27	8.59	9.42	7.24	8.87	13.3	16.3	10.4	9.52	9.94	7.24	9.68	9.61	0.94
Zr	52.9	49.9	55.0	21.6	42.8	70.0	80.5	36.6	28.5	13.4	18.3	21.3	21.3	56.7
Sm	2.80	3.03	2.99	2.44	3.04	4.01	4.52	3.00	2.03	1.98	1.57	1.99	1.91	0.57
Eu	1.02	1.05	1.03	0.88	1.03	1.25	1.61	1.13	0.53	0.49	0.40	0.48	0.42	0.27
Ti	8974	11140	10311	3993	8049	9558	10723	6846	1800	2554	2193	2555	1980	4894
Dy	2.41	2.56	2.33	2.40	2.49	2.91	3.31	2.75	1.05	1.10	0.95	1.15	1.04	2.74
Y	8.24	8.83	10.00	10.1	7.84	10.00	10.33	9.85	3.71	3.87	3.53	3.74	3.43	20.4
Er	0.96	0.93	0.61	0.90	0.78	1.07	1.07	1.10	0.41	0.43	0.37	0.42	0.37	2.30
Yb	0.66	0.66	0.24	0.52	0.69	0.98	1.02	0.92	0.39	0.38	0.36	0.43	0.30	2.83
Cr	99.8	119			324	101	87.1	125	935	1847	2140	1752	845	661

[1]After Ashchepkov and Andre, 2002.

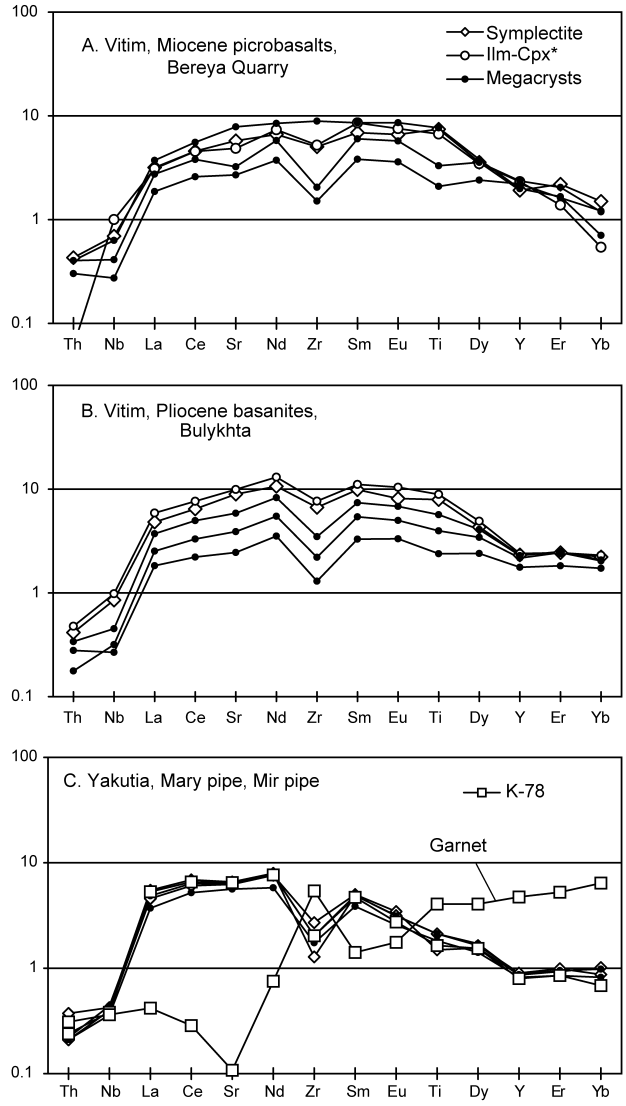

FIG. 7. Trace-element patterns of clinopyroxene from the Ilm-Cpx symplectites, Ilm-Cpx common intergrowths (Ilm-Cpx*), and megacrysts, normalized to primitive mantle after McDonough and Sun (1995).

for ilmenite plates in the symplectites were higher (900–1025°C), than those for common Ilm-Cpx intergrowths (830–950°C) and discrete ilmenite megacrysts (690–920°C) (Fig. 10, Table 5). The ranges of fO_2 for Ilm-Cpx symplectites and ilmenite megacrysts are generally similar ($fO_2 = 10^{-12.9}$ to $10^{-19.2}$, which is 0.22–1.88 logarithmic units lower than the QFM buffer, Fig. 10). These fO_2 values are similar to those for the majority of spinel peridotite xenoliths of the Vitim field (Litasov and Taniguchi, 2002).

The estimated ilmenite-magnetite temperatures are well correlated with the single-clinopyroxene temperature defined using the Mercier (1980) thermometer. This geothermometer gives higher temperatures (>100°C) in comparison with the more precise two-pyroxene thermometers (Wells, 1977; Brey and Kohler, 1990) (Fig. 11). However, because of its consistency the Mercier thermometer was used for qualitative estimations. Temperatures calculated using ilmenite-clinopyroxene equilibrium

calibrated by Bishop (1980) were greatly scattered and were not considered further.

For clinopyroxene megacrysts, Mercier-based temperatures ranged from 1140 to 1450°C (Bereya) and 1180 to 1400°C (Bulykhta and other Pliocene basanite locations). For the Ilm-Cpx symplectites, the temperatures are 1190°C (Bereya) and 1200–1210°C (Bulykhta). Temperatures for secondary recrystallized clinopyroxenes from symplectites were estimated in the range 1120–1180°C (Bereya) and 1100–1170°C (Bulykhta). Common Ilm-CPx (±biotite) intergrowths correspond to temperatures of 1180–1220°C (Bereya) and 1120–1200°C (Bulykhta). Ilm-CPx symplectites give higher temperatures relative to common Ilm-Cpx intergrowths, but lower temperatures relative to the majority of the clinopyroxene megacrysts.

Estimates were also made for the garnet-bearing megacrystalline websterites from the Vitim picrobasalts (Litasov et al., 2000). For these garnet-bearing assemblages, therefore, it is possible to speculate about pressures for the Ilm-Cpx

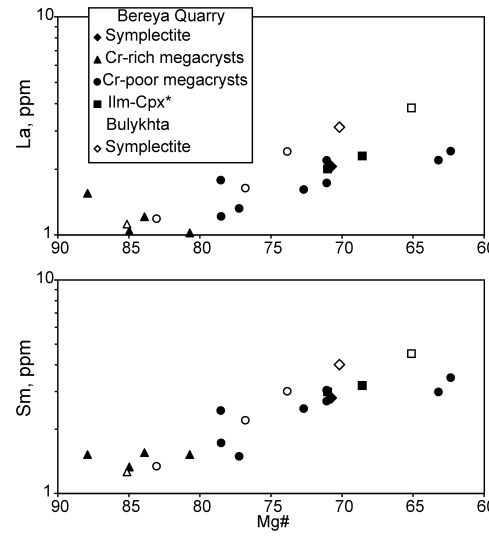

FIG. 8. Variations of REE (La and Sm) with Mg# in clinopyroxenes from the Ilm-Cpx symplectites and megacrysts of the Vitim field. Ilm-Cpx* represents common Ilm-Cpx intergrowths.

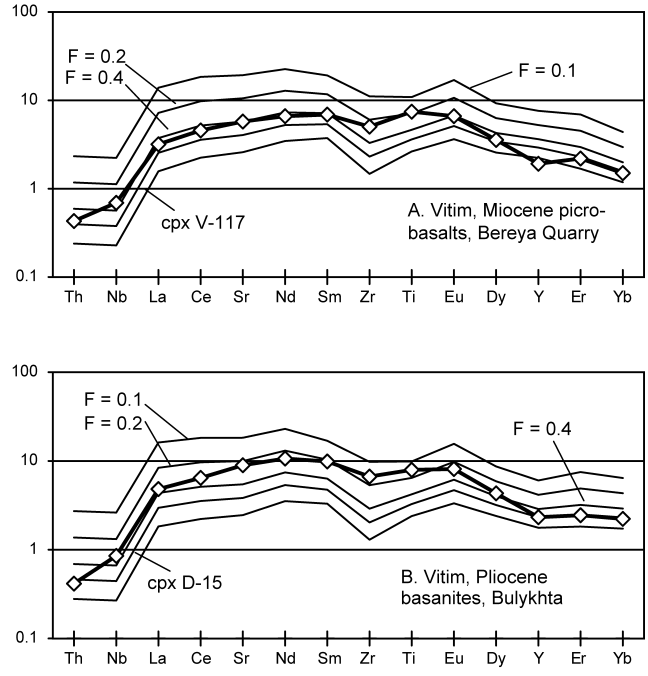

FIG. 9. Trace-element patterns of clinopyroxene, coexisiting with different melt fractions from modeling of fractional crystallization of the most primitive melt calculated from REE-poor clinopyroxene megacrysts from Miocene picrobasalts (V-117) and Pleistocene basanites (D-15) of the Vitim volcanic field. Symbols and abbreviations: diamonds = Ilm-Cpx-symplectites; F = fraction of residual melt. Cpx/melt partition coefficients for Th and Nb are from Hauri et al. (1994), and those for all other elements are from Hart and Dunn (1993). All data are normalized to primitive mantle after McDonough and Sun (1995). Data for V-117 and D-15 are from Litasov and Taniguchi (2002).

TABLE 5. TP-fO_2 Estimations for Ilm-Cpx Symplectites and Related Xenoliths

Sample	Type	T, °C	$\log fO_2$	$\Delta\log fO_2$ (QFM)
	T-fO2, ilmenite-magnetite (Anderson et al., 1993), Vitim, Bulykhta			
VBS-2	Ilm-Cpx symplectite	911	–13.5	–1.29
VBS-3	Ilm-Cpx symplectite	895	–14.4	–1.87
BK-25	Ilm-Cpx[1]	905	–12.8	–0.51
B-3	Megacryst	688	–19.2	–1.88
B-1	Megacryst	739	–17.3	–1.54

	T, °C			P, kbar
Type:	M-80	BK-90	EG-79	NG-85
	Vitim, Bereya picrobasalts			
Websterites, Cr-rich megacrysts	1340–1450	1220–1320	1200–1320	>30
Gt-websterites, Cr-poor	1260–1400	1150–1290	1102–1240	17–30
Cr-poor megacrysts	1140–1260			
Ilm-Cpx[1]	1180–1220			
Ilm-Cpx symplectites	1190			
	Vitim, Bulykhta (+others) basanites			
Cr-rich megacrysts	1380–1400			
Cr-poor megacrysts	1180–1350			
Ilm-Cpx[1]	1120–1200			
Ilm-Cpx symplectites	1200–1210			

Sample	Type	T, °C (EG-79)	T, °C (K-88)
		Kimberlites, Mir pipe	
K-78	Gt-symplectite	1062	979
A-702	Gt-symplectite	937	807
	Gt-Cpx[1]	920–1075	830–1000

[1]Common Ilm-Cpx and Gt-Cpx intergrowth. Thermometers: M-80 = Mercier, 1980, single-clinopyroxene for garnet stability field; BK-90 = Cpx-Opx, Brey and Kohler, 1990; EG-79 = Gt-Cpx, Ellis and Green, 1979; K-88 = Gt-Cpx, Krogh, 1988; NG-85 = Nickel and Green, 1985, garnet-orthopyroxene barometer.

symplectites. The geotherm derived from megacrystalline garnet websterites is hotter than that for garnet lherzolites from the same location, indicating partial disequilibrium with the surrounding mantle at the time of xenolith entrainment. Projections of the symplectite temperatures (T, Mercier, 1980, minus 100°C) on the geotherm derived from megacrystalline garnet websterites correspond to pressures of 12–17 kbar (Fig. 12).

It is more difficult to estimate P and T for the Ilm-Cpx symplectite from kimberlites, because the Mercier (1980) thermometer gives scarce or

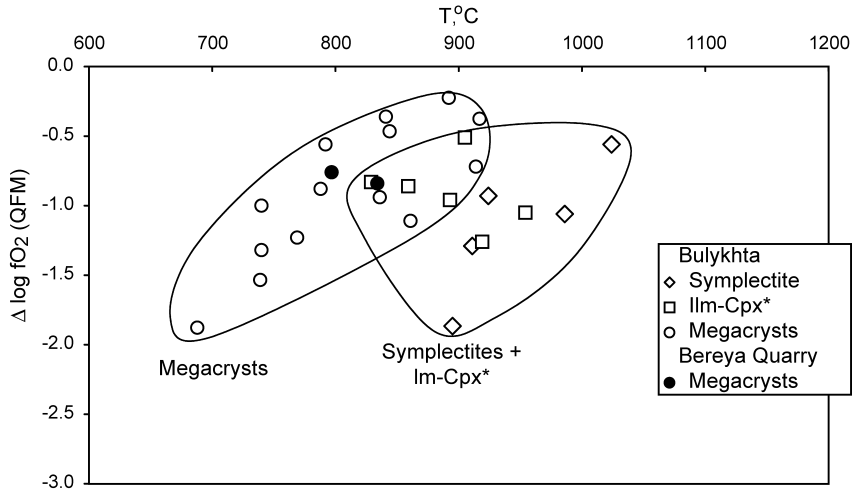

FIG. 10. T-fO_2 parameters calculated for ilmenite-magnetite exsolution pairs in the megacrysts and Ilm-Cpx symplectites of the Vitim field. Ilm-Cpx* represents common Ilm-Cpx intergrowths. Abbreviations: QFM = quartz-fayalite-magnetite buffer.

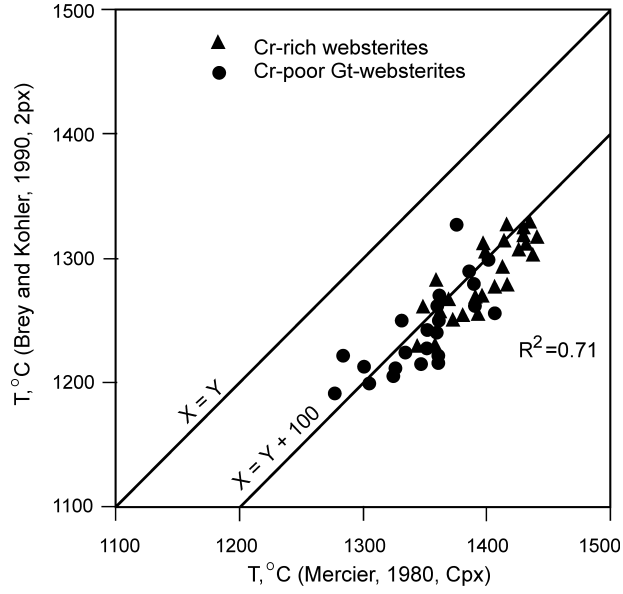

FIG. 11. Comparison between temperatures calculated by the two-pyroxene thermometer of Brey and Kohler (1990) with those by the single-clinopyroxene thermometer of Mercier (1980) for megacrystalline websterites from Bereya picrobasalts, Vitim field.

unrealistic results for kimberlite clinopyroxenes. Experiments by Wyatt (1977) supposed ilmenite-clinopyroxene co-precipitation out a wide range of temperatures (1250–1550°C) and pressures (20–47 kbar). Gurney et al. (1973) noted pressures between 50 and 60 kbar at about 1200°C in the zone of relative Ti-enrichment proposed by Boyd and Nixon (1973).

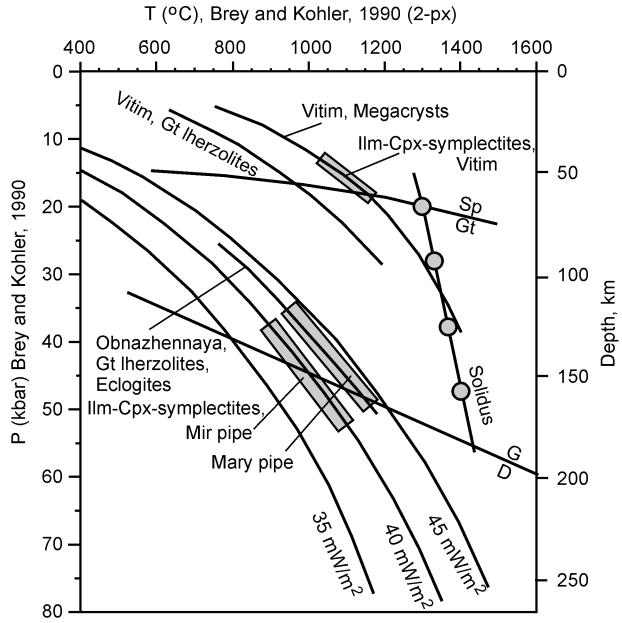

FIG. 12. P-T estimates for Ilm-Cpx symlectites. The geotherm for the Mir pipe coincides with the continental geotherm with a heat flow of 40 mW/m^2 (Roden et al., 1999). The geotherm for the Obnazhennaya pipe (assumed to be similar to the Mary pipe geotherm) is after Taylor et al. (2003). Continental geotherms with heat flows of 35, 40, and 45 mW/m^2 are based on data by Pollack and Chapman (1977). Solidus line and experimental points (circles) for melting experiments with a starting composition of the Ilm-Cpx symplectite are shown (Wyatt, 1977). Sp/Gt = spinel lherzolite to garnet lherzolite transition; G/D = graphite to diamond transition.

P-T estimates for garnet peridotites of the Mir pipe define a geotherm corresponding to a heat flow of 40 mW/m^2 (e.g., Pearson et al., 1995; Roden et al., 1999). Garnet-clinopyroxene temperatures for Gt-bearing symplectites of the Mir pipe fall within the temperature range for common megacrystalline, garnet-clinopyroxene intergrowths (910–1075°C, unpubl. data, Table 5). Therefore, assuming these temperatures of equilibration, possible pressures lie between 40 and 50 kbar (Fig. 12).

There is no geotherm constructed for the Mary pipe, but we suggest that it is similar to that for the nearby (Upper Jurassic) Obnazhennaya pipe of similar age (see review by Griffin et al., 1999). The geotherm of the Obnazhennaya pipe (Taylor et al., 2003) is of slightly higher temperature relative to that of the Mir pipe (Fig. 12). We have not calculated temperatures for ilmenite-clinopyroxene xenoliths from the Mary pipe because garnet-clinopyroxene intergrowths are absent. However, we suggest that the pressure range for the Ilm-Cpx symplectites is comparable to that of the Mir pipe based on the similarity in clinopyroxene compositions.

Discussion

The early hypotheses by Ringwood and Lovering (1970) and Dawson and Reid (1970) that Ilm-Cpx symplectites and rare ilmenite-orthopyroxene and ilmenite-garnet symplectites represent exsolution products from ultrahigh-pressure Ti-rich garnet or pyroxene were generally rejected after additional studies by Boyd and Nixon (1973), Gurney et al. (1973), and finally after the experimental work by Wyatt (1977). In this last study, the possibility of eutectic precipitation of clinopyroxene and ilmenite was demonstrated following clinopyroxene-only crystallization. The initial composition of Ilm-Cpx symplectite formed at 20–47 kbar. Wyatt (1977) determined that the liquidus phase is clinopyroxene followed by clinopyroxene + ilmenite.

Although Mitchell (1977) found that both major- and trace-element data do not indicate a simple relationship between megacrysts and symplectites. However, Garrison and Taylor (1981) felt that these two suites were related genetically and related to possible fractional crystallization of a "proto-

kimberlitic" or basaltic melt based on the compositional similarity of symplectite minerals and discrete megacrysts. In most kimberlite suites, the Mg# of clinopyroxene decreases sequentially from discrete megacrysts to Ilm-Cpx symplectites and then to Ilm-Cpx common intergrowths. In turn, the $MgTiO_3$ content in ilmenite decreases from symplectites to Ilm-Cpx common intergrowths and then to discrete megacrysts (e.g., megacryst suites of Monastery; Gurney et al., 1979; Lekkerfontein kimberlite; Robey and Gurney, 1979; Mir and Mary pipes, this work). Assuming the Mg# of minerals decrease during fractional crystallization, we argue that Ilm-Cpx symplectites crystallized after the major part of clinopyroxene megacrysts formed and before the majority of ilmenite megacrysts grew, marking the beginning stage of ilmenite precipitation from the liquid (see also, the review by Mitchell, 1986).

Frick (1973) discussed eutectic crystallization versus cotectic crystallization of ilmenite-silicate symplectites and concluded that cotectic precipitation best explains symplectite occurrences. It was thought to be difficult to explain both Ilm-Cpx and Ilm-orthopyroxene symplectites by eutectic crystallization from the same (proto-kimberlite or basaltic) liquid. Additionally, the majority of ilmenite megacrysts and common Ilm-Cpx intergrowths are likely to be crystallized from the same liquid after the crystallization of symplectites. Therefore, the join ilmenite-clinopyroxene is probably pseudobinary rather than a binary eutectic as proposed by Wyatt (1977).

Two groups of symplectites from the Mary pipe (Kostrovitsky and Piskunova, 1989 and references therein) reveal the following: (1) repeated pulses of melt from the depth; or (2) different magmatic events for their origin. Trace-element data indicate that the parental melt for symplectites of groups 1 and 2 should be quite similar in composition, whereas Cr-enrichment in symplectites of group 1 may reflect contamination by surrounding peridotites.

We have reported the first finding of Ilm-Cpx symplectites from alkaline basalts; this suggests a direct connection between symplectite crystallization and basaltic melt. Ilm-Cpx-symplectites in Vitim alkaline basalts are undoubtedly related to the megacryst assemblage, and formed during fractional crystallization from basaltic liquid at depth. Clinopyroxene is a major liquidus phase in alkaline basalt at 13–30 kbar (Thompson, 1974). The Mg# decrease of the melt and crystallizing phases and increase of alkalies, TiO_2, Al_2O_3, and REE in the residual liquid occurs during polybaric fractionation (Irving, 1974).

In the Vitim field, megacryst assemblages in Miocene picrobasalt from the Bereya Quarry include discrete nodules, as well as many mineral intergrowths and related pegmatitic-grained pyroxenites (Litasov et al., 2000). Parental melt for the megacrysts was estimated to be similar to that of the host picro-basalt. This melt was partially contaminated by surrounding lherzolites, at depth (>30 kbar), producing hybrid Cr-rich websterites. Compositional variations indicate the possibility of the following crystallization sequence, with decreasing temperature, pressure (Table 5), and Mg# of phases (Fig. 5): (1) clinopyroxene + orthopyroxene (Cr-rich websterites and clinopyroxenites); (2) clinopyroxene + orthopyroxene + garnet (nos. 2–7 are Cr-poor megacrysts and related pyroxenites); (3) clinopyroxene + garnet; (4) clinopyroxene only; (5) clinopyroxene + Ti-biotite; (6) clinopyroxene + ilmenite ± Ti-biotite (including Ilm-Cpx-symplectites); (7) clinopyroxene only. Residual melt, after megacrysts precipitation, penetrated into the lower crust where (8) garnet-bearing gabbros and clinopyroxenites were formed (Litasov et al., 2000). The crystallization sequence of megacryst phases in Pliocene basanites of Bulykhta is: (1) clinopyroxene; (2) clinopyroxene + garnet; (3) clinopyroxene; (4) clinopyroxene + ilmenite + Ti-biotite (including Ilm-Cpx-symplectites); and (5) ilmenite ± biotite (Litasov, 2000).

The role of ilmenite and biotite in the megacryst assemblages of Bulykhta basanites is more significant than that in Bereya megacrysts. This is because: (1) ilmenite and biotite megacrysts are abundant in Bulykhta and rare (biotite megacrysts are absent) in Bereya suites; and (2) modal abundances of ilmenite and biotite in the common intergrowth with clinopyroxene typically exceed 50% in the Bulykhta suite, whereas ilmenite and biotite occur as inclusions in clinopyroxene (usually <10 modal %) megacrysts in the Bereya suite.

Compositional variations in clinopyroxenes from Ilm-Cpx symplectites and megacrysts (Fig. 5) indicate that the Vitim symplectites crystallized after the majority of the clinopyroxene megacrysts and before the common Ilm-Cpx intergrowths and ilmenite megacrysts. This is the same as for the sequences in the kimberlite suites as noted above, consistent with cotectic crystallization of ilmenite

and clinopyroxene to form symplectites. Trace-element data support this idea and indicate that the compositions of clinopyroxene in symplectites are different from that expected for eutectic crystallization (Fig. 8).

P-T estimations show that Ilm-Cpx symplectites from Vitim alkaline basalts formed at shallower depths than those from kimberlites. Projections of temperatures on the geotherms derived from megacrystalline pyroxenites indicate pressures of 12–17 kbar. This is consistent with the experimental data by Wyatt (1977) that Ilm-Cpx symplectites can be crystallized from Ti-rich melt over a wide range of pressures (Fig. 12). The geotherm derived from megacrystalline garnet websterites in Bereya picrobasalts is hotter than that for garnet lherzolites from the same locale. This indicates thermal disequilibrium between the megacrysts and surrounding mantle peridotites. Therefore, polybaric formation of megacryst vein systems beneath the Vitim field occurred shortly before volcanic eruption and xenolith entrainment to the surface.

Deformation and recrystallization of symplectites was observed both in symplectites from basalts and kimberlites. In the Vitim symplectites, ilmenite recrystallization and grain enlargement retaining general crystallographic orientation inside clinopyroxene crystals were observed. This process may be associated with heating by late pulses of magma, probably with those that entrained samples to the surface.

A more complex history of symplectite recrystallization can be made for samples from the Mir pipe. It is obvious that formation of Ilm-Cpx symplectites in kimberlites is not connected with kimberlite eruptions. According to garnet-clinopyroxene thermometry, the Gt-bearing symplectites from the Mir pipe equilibrated at lower temperatures, corresponding to a continental geotherm with a heat flow of 40 mW/m_2 (constructed based on the garnet peridotite data, Fig. 12). However, the temperature of symplectite crystallization should be close to that of the experimental conditions in the Wyatt experiments (Fig. 12). Samples from the Mir pipe reveal several stages of superimposed metasomatism, resulting in grain enlargement, recrystallization, and formation of garnet, after primary crystallization of the Ilm-Cpx symplectite.

The sequence of transformation processes after crystallization of Ilm-Cpx symplectite for sample K-78 can be summarized as follows: (1) recrystallization and enlargement of ilmenite plates; (2) formation of garnet from metasomatic fluids, related deformation, and cataclasis of the symplectite; and (3) late metasomatic reactions and formation of reactionary phlogopite rims around garnet and rutile rims around ilmenite.

Conclusions

1. We have presented new findings regarding ilmenite-clinopyroxene symplectites in the Miocene picrobasalts and Pleistocene basanites of the Vitim volcanic field. For comparison, we have described both the typical and unusual ilmenite-clinopyroxene symplectites from kimberlites (the Mary pipe, the Kuoisk field, and the Mir pipe, Malo-Botuobinsk field, Yakutia), where this type of xenolith is more abundant.

2. Symplectite clinopyroxene from Vitim alkaline basalts corresponds to the low-Mg end of the clinopyroxene megacryst compositional trend. Megacryst assemblages of the Vitim field formed by continuous polybaric fractionation of basaltic melt. The beginning of ilmenite precipitation is indicated by an inflection on a TiO_2 versus Mg# trend in variation diagrams for clinopyroxene. Trace-element patterns of clinopyroxene from Vitim symplectites are more evolved (Lan = 3.1–3.8, normalized to primitive mantle) relative to the majority of megacrysts (Lan = 1.0–3.8). Modeling of fractional crystallization of clinopyroxene from an alkaline basaltic melt indicates that clinopyroxenes from symplectites correspond to the residual melt fraction of 20–40%, generally too high to be eutectic crystallization.

3. Symplectites from kimberlites of the Mary pipe can be divided into Cr-rich and Cr-poor subgroups. However, trace-element patters are similar for clinopyroxenes from both groups. This may indicate a symplectite origin by repeated pulses of magma. Cr-enrichment for the Cr-rich group can be attributed to metasomatic contamination from adjacent peridotites.

4. Compositional and textural variations in symplectites from both alkaline basalts and kimberlites reveal the similarity of their genesis and a clear connection with megacryst assemblages. We suggest that ilmenite-clinopyroxene symplectites characterize the initial stage of simultaneous precipitation of ilmenite and clinopyroxene in both kimberlites and alkaline basalts. This takes place after the majority of clinopyroxene megacryst has crystallized, when Ti-enrichment of the residual melt exceeds a certain threshold, and before growth of the common

Ilm-Cpx intergrowths and ilmenite megacrysts. This supports cotectic rather than eutectic crystallization of ilmenite and clinopyroxene to form the symplectites.

5. Estimation of P-T parameters for garnet-bearing Ilm-Cpx symplectites from the Mir pipe indicates that symplectite from kimberlite possibly formed at pressures of 40–50 kbar, whereas those from Vitim basalts formed at only 12–17 kbar. Coexisting Fe-Ti oxides in Vitim ilmenites from symplectites and megacrysts suggest equilibration temperatures of 690–1025°C at fO_2 = 0.22–1.88 log units below the QFM buffer curve. This redox state resembles that of spinel peridotites at the same localities.

Acknowledgments

The senior author acknowledges the Center for Northeast Asian Studies (CNEAS), Tohoku University and the Japan Society for Promotion of Sciences (JSPS) for research fellowships. Portions of the research for this study was supported by the Russian Foundation for Basic Research grants (no. 97-05-65309) and NSF Grant EAR 99-09543 (LAT).

REFERENCES

Anderson, D. J., Lindsley, D. H., and Davidson, P. M., 1993, QUILF: A Pascal program to assess equilibria among Fe-Mg-Mn-Ti oxides, pyroxenes, olivine and qartz: Computers and Geoscience, v. 19, p. 1333–1350.

Ashchepkov, I. V., and Andre, L., 2002, Pyroxenite xenoliths in picrite basalt (Vitim plateau): Origin and differentiation of mantle melts: Russian Geology and Geophysics, v. 43, p. 343–363.

Batanova, V. G., Suhr, G., and Sobolev, A. V., 1998, Origin of geochemical heterogeneity in the mantle peridotites from the Bay of Islands ophiolite, Newfoundland, Canada: Ion probe study of clinopyroxenes: Geochimica et Cosmochimica Acta, v.62, p.853–866.

Bishop, F. C., 1980, The distribution of Fe^{2+} and Mg between coexisting ilmenite and pyroxene with applications to geothermometry: American Journal of Science, v. 280, p. 46–77.

Boyd, F. R., and Nixon, P. H., 1973, Origin of the ilmenite-silicate nodules in kimberlites from Lesotho and South Africa *in* Nixon, P., ed., Lesotho kimberlites: Cape Town, South Africa, Cape and Transvaal Printers Ltd., p. 254–268.

Brey, G. P., and Köhler, T., 1990, Geothermobarometry in four-phase lherzolites II. New thermobarometers, and practical assessment of existing thermobarometers: Journal of Petrology, v. 31, p. 1313–1336.

Dawson, J. B., and Reid, M. A., 1970, Pyroxene-ilmenite intergrowth from the Monastery mine South Africa: Contributions to Mineralogy and Petrology, v. 26, p. 296–301.

Delaney, J. S., Smith J. V., Carswell D. A., and Dawson, J. B., 1980, Chemistry of micas from kimberlites and xenoliths—II. Primary- and secondary-textured micas from peridotite xenoliths: Geochimica et Cosmochimica Acta, v. 44, p. 857–872.

Ehrenberg, S. N., 1982, Petrogenesis of garnet lherzolite and megacrystalline nodules from the Thumb, Navajo Volcanic Field: Journal of Petrology, v. 23, p. 507–547.

Ellis, D. J., and Green, D. H., 1979, An experimental study of the effect of Ca upon garnet-clinopyroxene Fe-Mg exchange equilibria: Contributions to Mineralogy and Petrology, v. 71, p. 13–22.

Frick, C., 1973, Intergrowths of orthopyroxene and ilmenite from Frank Smith Mine, near Rarkly West, South Africa: Transactions of the Geological Society of South Africa, v. 76, p. 195–200.

Garrison, J. R., and Taylor, L. A., 1981, Petrogenesis of pyroxene-oxide intergrowths from kimberlite and cumulate rocks: Co-precipitation or exsolution?: American Mineralogist, v. 66, p. 723–740.

Griffin, W. L., Ryan, C. G., Kaminsky, F. V., O'Reilly, S. Y., Natapov, L. M., Win, T. T., Kinny, P. D., and Ilupin, I. P., 1999, The Siberian lithosphere traverse: Mantle terranes and the assembly of the Siberian Craton: Tectonophysics, v. 310, p. 1–35.

Gurney, J. J., Fesq, H. W., and Kable, J. D., 1973, Clino/pyroxene-ilmenite intergrowth from kimberlite: A re-appraisal, *in* Nixon, P., ed., Lesotho kimberlites: Cape Town, South Africa, Cape and Transvaal Printers Ltd., p. 238–253.

Gurney, J. J., Jakob, W. R. O., and Dawson, J. B., 1979, Megacrysts from the Monastery kimberlite pipe, South Africa, *in* Boyd, F. R., and Meyer, H. O. A., eds., The mantle samples: Inclusions in kimberlites and other volcanics, *in* Proceedings of the Second International Kimberlite Conference, p. 227–243.

Hart, S. R., and Dunn, T., 1993, Experimental cpx/melt partitioning of 24 trace elements: Contributions to Mineralogy and Petrology, v. 113, p. 1–8.

Hauri, E. H., Wagner, T. P., and Grove, T. L., 1994, Experimental and natural partitioning of Th, U, Pb, and other trace elements between garnet, clinopyroxene and basaltic melts: Chemical Geology, v. 117, p. 149–166.

Ionov, D. A., Ashchepkov, I. V., Stosch, H.-G., Witt-Eickschen, G., and Seck, H. A., 1993, Garnet peridotite xenolith from the Vitim volcanic field, Baikal region: The nature of the garnet-spinel peridotite transition

zone in the continental mantle: Journal of Petrology, v. 34, p. 1141–1175.

Irving, A. J., 1974, Megacrysts from the Newer Basalts and other basaltic rocks of south-eastern Australia: Geological Society of America Bulletin, v. 85, p. 1503–1514.

Kostrovitsky, S. I., Klopotov, V. I., Garanin, V. K., and Serenko, V. P., 1992, Ilmenite-clinopyroxene symplectite with garnet from the Mir pipe: Proceedings of the Russian Mineralogical Society, v. 2, p. 47–54 (in Russian).

Kostrovitsky, S. I., and Piskunova, L. F., 1989, Two groups of symplectites from one kimberlite pipe: Transactions (Doklady) Russian Academy of Sciences, v. 306, p. 1213–1216.

Krogh, E. J., 1988, The garnet-clinopyroxene Fe-Mg geothermometer—a reinterpretation of existing experimental data: Contributions to Mineralogy and Petrology, v. 99, p. 44–48.

Litasov, K. D., 2000, Petrology of a megacrysts assemblage in Plio-Pleistocene basanites from the Vitim Plateau: Volcanology and Seismology, v. 22, no. 1, p. 24–35.

Litasov, K. D., and Ashchepkov, I. V., 1996, Ilmenite megacrysts and ilmenite-bearing pyroxenites from alkaline basalts, Vitim Plateau: Russian Geology and Geophysics, v. 37, p. 97–108.

Litasov, K. D., Foley, S. F., and Litasov, Yu. D., 2000, Magmatic modification and metasomatism of the subcontinental mantle beneath the Vitim volcanic field (East Siberia): Evidence from trace element data on pyroxenite and peridotite xenoliths from Miocene picrobasalt: Lithos, v. 54, p. 83–114.

Litasov, K. D., Kostrovitsky, S. I., and Litasov, Yu. D., 1998, Comparison of ilmenite-clinopyroxene symplectites from Vitim alkaline basalts and Yakutian kimberlites (Siberia, Russia) [ext. abs.]: Extended abstracts of the Seventh International Kimberlite Conference, Cape Town, South Africa, p. 503–505.

Litasov, K. D., and Litasov, Yu. D., 1999a, Petrology of garnet-spinel lherzolites and accompanyng xenoliths from Pliocene-Pleistocene basanites of the Vitim volcanic plateau: Russian Geology and Geophysics, v. 40, p. 546–558.

_____, 1999b, Biotite in megacryst assemblages of the alkaline basaltoids, Vitim plateau: Geochemistry International, v. 37, p. 213–223.

Litasov, K. D., and Taniguchi, H., 2002, Mantle evolution beneath the Baikal rift: CNEAS Monograph Series, v. 5, Tohoku University, Sendai, Japan, 223 p.

McDonough, W. F., and Sun, S. S., 1995, The composition of the Earth: Chemical Geology, v. 120, p. 223–253.

Mercier, J. C. C., 1980, Single-pyroxene thermobarometry: Tectonophysics, v. 70, p. 1–37.

Mitchell, R. H., 1977, Geochemistry of magnesian ilmenites from kimberlites from South Africa and Lesotho: Lithos, v. 10, p. 29–37.

_____, 1986, Kimberlites: Mineralogy, geochemistry and petrology. New York, NY, Plenum Publishing Company, 442 p.

Nickel, K. G., and Green, D. H., 1985, Empirical geothermobarometry for garnet peridotites and implications for the nature of the lithosphere, kimberlites and diamonds: Earth and Planetary Science Letters, v.73, p. 158–170.

Nixon, P. H., and Boyd, F. R., 1979, Garnet-bearing lherzolites and discrete nodules from the Malaita alnoite, Solomon Islands, S.W. Pacific, and their bearing on oceanic mantle composition and geotherm, *in* Boyd, F. R., and Meyer, H. O. A., eds., The mantle samples: Inclusions in kimberlites and other volcanics: Proceedings of the Second International Kimberlite Conference, p. 400–423.

Pearson, D. G., Shirey, S. B., Carlson, R. W., Boyd, F. R., Pokhilenko, N. P., and Shimizu, N., 1995, Re-Os, Sm-Nd, and Rb-Sr isotope evidence for thick Archaean lithospheric mantle beneath the Siberian craton modified by multistage metasomatism: Geochimica et Cosmochimica Acta, v. 59, p. 959–977.

Pollack, H. N., and Chapman, D. S., 1977, Mantle heat flow: Earth and Planetary Science Letters, v. 34, p. 174–184.

Ponomarenko, A. I., 1977, Genesis of ilmenite-clinopyroxene intergrowths (xenoliths from kimberlite pipes): Transactions (Dokaldy) of the Russian Academy of Sciences, v. 235, p. 1162–1165.

Ringwood, A. E., and Lovering, J. F., 1970, Significance of pyroxene-ilmenite intergrowths among kimberlite xenoliths: Earth and Planetary Science Letters, v. 7, p. 371–375.

Robey, J. V. A., and Gurney, J. J., 1979, Megacrysts from the Lekkerfontein kimberlite, North central Cape, R.S.A [ext. abs.]: Extended abstracts, Kimberlite Symposium II, Cambridge, UK.

Roden, M. F., Laz'ko, E. E., and Jagoutz, E., 1999, The role of garnet pyroxenites in the Siberian lithosphere: Evidence from the Mir kimberlite, *in* Gurney, J., et al. eds., Proceedings of the Seventh International Kimberlite Conference, Cape Town, v. 2, p. 714–720.

Shimizu, N., and Hart, S. R., 1982, Isotope fractionation in secondary ion mass spectrometry: Journal of Applied Physics, v. 53, p. 1303–1311.

Shulze, D. J., 1987, Megacrysts from alkaline volcanic rocks, *in* Nixon, P., ed., Mantle xenoliths: New York, NY, John Wiley, p. 433–452.

Sobolev, A. V., Migdisov, A. A., and Portnyagin, M. V., 1996, Incompartible elements partitioning between clinopyroxene and basaltic melt based on the study of melt inclusions in minerals from Troodos, Cyprus: Petrology, v. 4, p. 307–317.

Sobolev, N. V., and Nixon, P. H., 1987, Xenoliths from the USSR and Mongolia: A selective and brief review, *in* Nixon, P., ed., Mantle xenoliths: New York, NY, Wiley, p. 159–165.

Solovyova, L. V., Vladimirov, B. M., Dneprovskaya, L. V., and Maslovskaya, M. N., 1994, Kimberlites and kimberlite-like rocks: Upper mantle beneath the ancient cratons: Novosibirsk, Russia, Nauka Press, 320 p. (in Russian).

Taylor, L. A., Snyder, G. A., Keller, R., Remley, D. A., Anand, M., Wiesli, R., Valley, J., and Sobolev, N. V., 2003, Petrogenesis of group A eclogites and websterites: Evidence from the Obnazhennaya kimberlite, Yakutia: Contributions to Mineralogy and Petrology, v. 145, p. 424–443.

Thompson, R. N., 1974, Some high-pressure pyroxenes: Mineralogical Magazine, v. 39, p. 768–787.

Wells, P. R. A., 1977, Pyroxene thermometry in simple and complex systems: Contributions to Mineralogy and Petrology, v. 62, p. 129–139.

Wyatt, B. A., 1977, The melting and crystallization behavior of a natural clinopyroxene-ilmenite intergrowth: Contributions to Mineralogy and Petrology, v. 61, p. 1–9.